Autofrettage of Open-End Tubes—Pressures, Stresses, Strains, and Code Comparisons

Anthony P. Parker
Engineering Systems Department,
Royal Military College of Science,
Cranfield University,
Swindon, England
e-mail: tony_parker@tesco.net

Autofrettage is used to introduce advantageous residual stresses into pressure vessels. The Bauschinger effect can produce less compressive residual hoop stresses near the bore than are predicted by ''ideal'' autofrettage solutions. A recently developed numerical analysis procedure is adopted and extended. The ratio of calculated autofrettage pressure (numerical)/ideal autofrettage pressure (Tresca criterion and plane stress) is calculated and verified against available solutions. The case of open-end conditions based upon von Mises and engineering plane strain (constant axial strain with zero net axial force) is examined in detail. The ratio in this case varies between unity and $2/\sqrt{3}$, but exhibits very significant variations from the plane stress case when the diameter ratio of the tube exceeds 1.8. Results are within 0.5 percent of available analytical, numerical, and experimental results. A simple numerical fit allows all autofrettage pressures to be replicated to within 0.5 percent. The true plane strain pressure ratio is examined and shown to be inappropriate in modeling engineering plane strain. A number of residual hoop and axial stress profiles is presented for radius ratio 2.0. Calculated pressures are used to determine residual hoop stress values for tube diameter ratios from 1.1 to 3.0 for the full range of percentage overstrain levels. These comparisons indicate that Bauschinger effect is evident when the ratio autofrettage radius/bore radius exceeds 1.2, irrespective of diameter ratio. To assist designers the important values of residual hoop stress at the bore are summarized in a composite plot and a numerical fit is provided. The accuracy of the current ASME code using pressure criteria is assessed. The code is shown to be generally and modestly conservative. A design procedure is proposed which appears capable of extending code validity beyond 40 percent overstrain (the limit of the current code) and of eliminating the small nonconservatism at very low overstrain. Hoop strain values are calculated at both the bore and outside diameter of a tube of radius ratio 2 at the peak of the autofrettage cycle using von Mises criterion with open-end, closed-end, and plane strain conditions. These are compared with available solutions; general agreement is demonstrated, with agreement within 2 percent with an accepted simple formula in the case of open ends. ASME code predictions of percentage overstrain based upon strains at the peak of the autofrettage cycle are generally within 6 percent of numerical predictions. This is in turn produces an agreement within approximately 3 percent in residual bore hoop stress calculation. This discrepancy is generally conservative, becoming non-conservative only at overstrain levels exceeding 80 percent. Strain during removal of autofrettage pressure, in the presence of Bauschinger effect, is also calculated. This shows that the difference in strain during the unloading phase is up to 8 percent (ID) and 6.3 percent (OD) compared with the predictions of elastic unloading. These latter results show similar agreement with the ASME code as in the peak-strain analysis and permit correction of estimates of percentage overstrain based upon permanent bore enlargement.
[DOI: 10.1115/1.1359209]

Introduction

Autofrettage is used to introduce advantageous residual stresses into pressure vessels and to enhance their fatigue lifetimes. For many years workers have acknowledged the probable influence of the Bauschinger effect [1], which serves to reduce the yield strength in compression as a result of prior tensile plastic overload. Chakrabarty [2] provides some review of the microstructural causes.

The reduction of compressive yield strength within the yielded zone of an autofrettaged tube is of importance because, on removal of the autofrettage pressure, the region near the bore experiences high values of compressive hoop stress, approaching the magnitude of the tensile yield strength of the material, if the unloading is totally elastic. If the combination of stresses exceeds some yield criterion, the tube will reyield from the bore, thus losing much of the potential benefit of autofrettage.

This work employs the numerical procedure proposed by Jahed and Dubey [3] and further developed, together with a review of previous work [4]. The aims are to determine:

(a) pressure to achieve a given percentage overstrain
(b) residual stress profiles
(c) bore hoop residual stress values
(d) simple, accurate numerical fits to (a) and (c)
(e) strains at ID and OD after autofrettage pressurization
(f) strains at ID and OD after autofrettage depressurization
(g) comparisons with relevant sections of the ASME code

The following geometrical definitions apply (see Fig. 1): Tube inner radius, a; tube outer radius, b; radius of plastic zone at peak of autofrettage cycle, c; maximum radius of reversed plasticity, d;

Contributed by the Pressure Vessels and Piping Division and presented at the Pressure Vessels and Piping Conference, Seattle, Washington, July 23–27, 2000, of THE AMERICAN SOCIETY OF MECHANICAL ENGINEERS. Manuscript received by the PVP Division, April 15, 2000; revised manuscript received November 24, 2000. Associate Editor: D. M. Fryer.

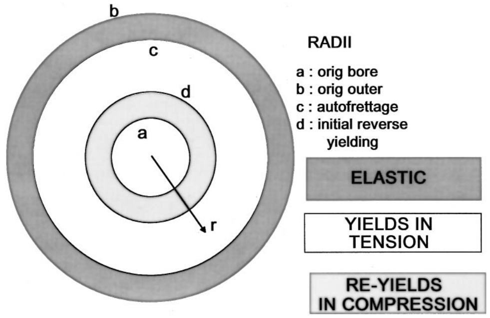

Fig. 1 Tube geometry

general radius location, r. Overstrain is defined as the proportion of the wall thickness of the tube which behaves plastically during the initial application of autofrettage pressure.

The materials considered are steels which conform with the descriptions contained within [5], upon which the uniaxial stress-strain behavior in tension and subsequent compression is based. The materials reported in [5] do not exceed a yield strength of 1100 MPa; there is also good reason to believe that this behavior also extends to martensitic steels having significantly higher yield strengths [6].

Parker et al. [4] present typical hoop residual stress profiles based upon a Tresca criterion plane stress analysis arising from autofrettage of a tube of radius ratio 2.0. The ''ideal'' profile for elastic-perfectly plastic behavior without Bauschinger effect is included for comparison. Noteworthy effects include:

- Large reduction in bore hoop stress as a result of Bauschinger effect
- The Bauschinger effect penetrates much deeper into the tube than previous attempts at modeling typical gun steels have suggested: approximately 22 and 30 percent of wall thickness for overstrains of 60 and 100 percent, respectively, for a tube of radius ratio 2.0. Previous work has suggested depths of around 16 percent.
- A minimum value of hoop stress at the bore associated with a 'saturation' value of 2 percent plastic strain. This is a direct result of the constant Bauschinger effect factor (BEF) values observed by Milligan et al. [5] for plastic strain >2 percent.
- Very limited benefit (in terms of increased compressive hoop stresses in the near-bore region) as a result of overstrain above 60 percent.
- Disadvantages in autofrettage above 60 percent because of the significant increase in tensile residual hoop stress at the outside diameter.

The results presented in [4] all relate to Tresca's yield criterion under plane stress conditions and are limited principally to $b/a=2$. Work herein covers the range $1.1\leqslant b/a\leqslant 3.0$ and includes the more practically relevant case of von Mises' yield criterion combined with engineering plane strain (EPS) conditions, i.e., constant axial strain with zero net axial force, often referred to as open-end conditions. However, in order to simplify the presentation of results for such a large range of geometries and overstrain levels, attention is focused upon bore hoop stresses. These are of overriding importance because it is this value which dominates fatigue crack growth calculations and which is used to determine pressure for reyielding [4].

In order to achieve the aims it is necessary to critically examine certain common assumptions. The first of these is the frequent use of a multiplying factor of 1.15 $(2/\sqrt{3})$ in order to determine residual stress profiles based upon von Mises' criterion from those obtained using Tresca's criterion. The second, separate assumption is the use of a similar multiplying factor in determining the required bore pressure to achieve a given percentage overstrain. This factor is used to scale the autofrettage pressure determined via a Tresca plane stress analysis. For various reasons the combined effect of any error in these factors could far exceed the intuitive expectation of a maximum effect of 15 percent.

Previous work on strains in autofrettaged tubes with various combinations of end conditions and yield criteria has been reviewed and extended in [7]. A text containing a general overview and examples is available [2]. Further work is due to Marcal [8], who used a numerical stiffness method to determine OD strain as a function of peak autofrettage pressure; he also provided a plot of OD strain versus ID strain for a range of diameter ratios.

There does not appear to have been any previous numerical quantification of the influence of Bauschinger effect upon the strain during unloading (i.e. during removal of autofrettage pressure). It is usually assumed, in calculating strains, that such unloading is wholly elastic. Conversely, it is usually assumed, in calculating residual stresses, that such unloading does involve further plasticity. These assumptions are mutually incompatible. The inference of further plasticity during unloading is incontrovertible, and the question is therefore not whether unloading is inelastic, but whether such behavior makes any significant contribution to strain values and subsequent stress calculations.

The ASME Code [9] contains procedures for relating OD strain at peak autofrettage loading to the percentage overstrain. It also provides a method for relating the difference between bore diameter before and after autofrettage (termed permanent bore enlargement) to the level of overstrain.

In this paper strains are calculated for von Mises criterion applied to EPS, closed-end (constant axial strain with net axial force equal to internal pressure $\times$ bore cross-sectional area), and plane strain (zero axial strain) configurations.

Analysis Procedure

The residual compressive hoop stress within the plastically deformed region of an autofrettaged tube determined via a Tresca plane stress analysis without Bauschinger effect is well known [2], and is given by

$$\sigma_\theta]^{T\sigma}=-p]^{T\sigma}+Y[1+\ln(r/a)]-[p]^{T\sigma}a^2(b^2-a^2)]\cdot[1+b^2/r^2] \tag{1}$$

where Y is the uniaxial yield stress for the material, and the autofrettage pressure (Tresca, plane stress), $p]^{T\sigma}$ is given by

$$p]^{T\sigma}=Y[\ln(c/a)+(b^2-c^2)/2b^2] \tag{2}$$

and $c/a\leqslant 2.22$. Yielding onset (0 percent overstrain, $c=a$) occurs when

$$p]_{0\text{ percent}}^{T\sigma}=Y(b^2-a^2)/2b^2 \tag{3}$$

The equivalent pressure for the case of von Mises and plane stress, $p]_{0\text{ percent}}^{VM\sigma}$ [2], may be obtained from

$$p]_{0\text{ percent}}^{VM\sigma}/p]_{0\text{ percent}}^{T\sigma}=(2/\sqrt{3})/\sqrt{1+1/\{3(b/a)^4\}} \tag{4}$$

100 percent overstrain $(c=b)$, for Tresca, plane stress requires a pressure

$$p]_{100\text{ percent}}^{T\sigma}=Y\ln(b/a) \tag{5}$$

Substituting Eq. (2) into Eq. (1)

$$\sigma_\theta]^{T\sigma}/Y=(c^2+b^2)/2b^2+\ln(r/c)-[a^2/(b^2-a^2)]\cdot[1+b^2/r^2]\cdot[(b^2-c^2)/2b^2+\ln(c/a)] \tag{6}$$

The value of hoop stress at the bore is obtained by setting $r=a$ in Eq. (6) to give

$$\sigma_\theta]_{\text{bore}}^{T\sigma}/Y=[(c^2-a^2)-2b^2\ln(c/a)]/[b^2-a^2] \tag{7}$$

Hill [10] reviews approximate methods of correcting Eq. (7) to simulate von Mises criterion in modeling the autofrettage process. Hill concludes with the now familiar finding that by substituting $2Y/\sqrt{3}$ (generally represented as $1.15Y$) for Y in Eqs. (6) and (7), the errors in residual stress prediction are less than 2 percent. The implication is that for a given percentage overstrain, a simple scaling of the Tresca residual stress predictions by 1.15 will produce the desired von Mises prediction. Note that Hill's analysis implicitly excludes Bauschinger effect and assumes true plane strain conditions (TPS), i.e., zero axial strain. This will be of importance in understanding upcoming results relating to EPS.

The question of modification of autofrettage pressure to account for von Mises criterion with open-end conditions has been addressed by several workers. Davidson et al. [11] obtained experimental values of pressure at 100 percent overstrain in the range $1.6 \leqslant b/a \leqslant 2.4$, Marcal [8] employed a stiffness method and determined pressure for 100 percent overstrain in the range $1.5 \leqslant b/a \leqslant 4.0$, together with hoop strains at the outer surface for the complete range of possible overstrain pressures. Davidson and Kendall [7] proposed an empirical pressure value of $1.08Y \ln(b/a)$ for the case of 100 percent overstrain, with an associated maximum error of 2 percent. The current ASME pressure vessel code [9] uses a fixed scaling factor of $1.15p]^{T\sigma}$, but limits code validity to a maximum of 40 percent overstrain.

A rational approach to the numerical procedure, which is lengthy and often involves multiple iterations, requires that analyses are undertaken in a specific sequence, namely:

Step 1 For each tube geometry iteratively determine pressure to achieve a given percentage overstrain. This is repeated for the case of von Mises', plane stress, $p]^{VM\sigma}$, and von Mises, EPS $p]^{VMEPS}$. Both sets of results are normalized with Tresca, plane stress, $p]^{T\sigma}$. The first set is used to validate numerical results by comparison with analytical bounds, the second set is used as the basis of a proposed design procedure.

Step 2 Determine some simple numerical fit to the ratios determined in Step 1 for use by designers.

Step 3 Employ the autofrettage pressures determined in Step 1 for the von Mises, EPS case in determining a limited range of autofrettage residual stress profiles. These results to cover hoop and axial stress and encompass both Bauschinger-affected and non-Bauschinger-affected situations.

Step 4 Determine numerous bore hoop stress values for the von Mises, EPS case, normalized with $\sigma_\theta]^{T\sigma}$ from Eq. (1).

Step 5 Determine some simple numerical fit to the ratios determined in Step 4 for use by designers.

Step 6 Use procedures employed in Steps 1–5 to assess accuracy of ASME code.

Step 7 Propose a procedure which will improve accuracy and extend code validity beyond current 40 percent overstrain limit.

Step 8 Repeat appropriate steps to determine ID and OD strain values.

Pressure for Given Overstrain Level

Figure 2 shows numerically determined values of bore pressure for a given percentage overstrain based upon von Mises criterion, plane stress, $p]^{VM\sigma}$, normalized with the equivalent Tresca, plane stress pressure $p]^{T\sigma}$. Elastic-perfectly plastic behavior is assumed during loading. Two analytical bounds are also shown: the first is the onset of autofrettage as defined by Eq. (3), while the second bound relates to 100 percent overstrain and was obtained iteratively from Weigle [12]. This equation, in current notation, is

$$2 \ln\left[\frac{(b/a)^2\sqrt{3\gamma}}{1+\sqrt{3\gamma-3}}\right]=\sqrt{3}\pi-2\sqrt{3} \quad \arctan \quad \sqrt{\gamma-1} \tag{8}$$

where

$$\gamma=\frac{4}{3}\left[Y/(p]^{VM\sigma}_{100\ \text{percent}})\right]^2 \tag{9}$$

and, for a real solution

$$(p]^{VM\sigma}_{100\ \text{percent}})/Y \leqslant 2/\sqrt{3} \tag{10}$$

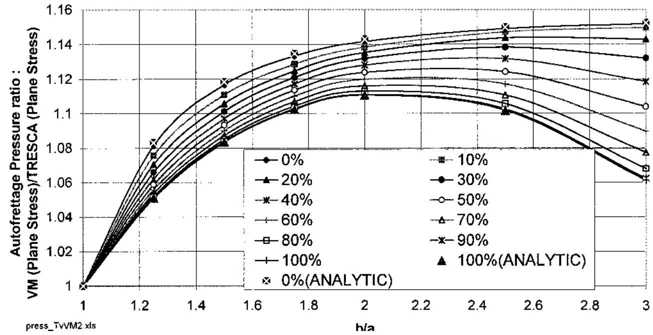

Fig. 2 Bore pressure for given percentage overstrain, von Mises and plane stress conditions assumed

The numerical results for the cases 0 and 100 percent overstrain are within 0.2 percent of the analytical bounds. The 100 percent bound is not valid beyond $b/a=2.5$ because of the restriction imposed by Eq. (10). Figure 2 gives considerable confidence in the numerical procedure employed. The technique is now extended to the case of von Mises, EPS.

The numerical procedure required to encompass EPS requires only one enhancement to the procedure employed thus far and described in [4]. This involves an additional iterative stage in which a true plane strain (TPS) (i.e., zero axial strain) solution is obtained initially and total axial force in the tube determined. An appropriate constant strain is then applied to the tube and iteratively adjusted until EPS is achieved. This extended procedure requires two alternating sets of iterations. It was found that each EPS solution for a given geometry and autofrettage pressure required around 1000 iterations in total; however, since the selection of autofrettage pressure for a given overstrain is itself iterative, this number must be factored by a further 10 or 20. Since the pressure-iteration procedure does not readily lend itself to complete automation, the process is undeniably time consuming! The scheme does nonetheless provide a monotonic, repeatable, mesh-independent convergence.

Figure 3 is in precisely the same format as Fig. 2, but relates to von Mises criterion, EPS solutions, $p]^{VMEPS}$. In this case the previous bounds are clearly in evidence, with 0 percent forming an excellent upper bound, but with significant deviation at $b/a > 1.5$, as might be anticipated, from the 100 percent von Mises, plane stress bound. The analytic TPS bound for 0 percent overstrain [2], labeled ''100 percent ANALYTIC,'' is also included. This leads to an important observation: the use of a fixed pressure ratio of $2/\sqrt{3}$ may be justifiable in the TPS case, but appears inappropriate in the EPS case.

The following expression provides a fit to the EPS (open-end) results which are generally within 0.5 percent over the entire range:

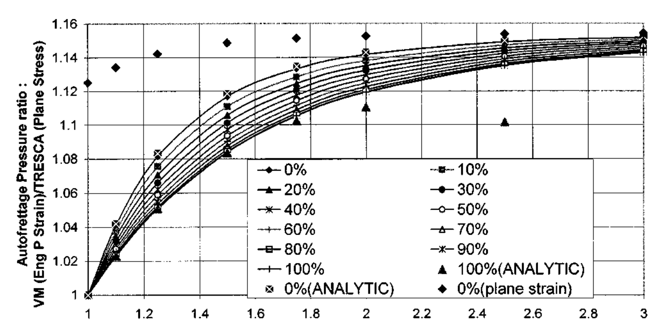

Fig. 3 Bore pressure for given percentage overstrain, von Mises and engineering plane strain (open-end) conditions assumed

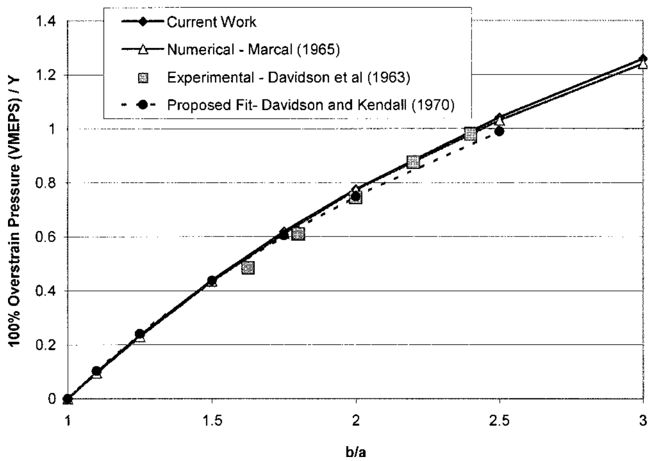

Fig. 4 Bore pressure for 100 percent overstrain—comparison with other work, von Mises and engineering plane strain conditions

$$\frac{p]^{\mathrm{VMEPS}}}{p]^{\mathrm{T}\sigma}}=\frac{(2/\sqrt{3})}{\sqrt{1+1/\{3(b/a)^{\alpha}\}}} \tag{11}$$

where

$$\alpha=4-2.3n \tag{12}$$

and

$$n=(c-a)/(b-a), \quad (c-a)/(b-a)\leqslant 70\text{ percent} \tag{13}$$

$$n=70\text{ percent}, \quad (c-a)/(b-a)>70\text{ percent} \tag{14}$$

The results for 100 percent overstrain with open ends may also be compared with two other sources. Figure 4 shows pressure for 100 percent overstrain normalized with yield stress. The results of Marcal [8] who used a numerical procedure are shown together with the averaged experimental results of Davidson et al. [11] and the empirical fit proposed by Davidson and Kendall [7]. The current work is within 1 percent of [8], and within 4 percent of the experimental results. The experimental results fall generally below the numerical. It was also noted that the outside surface hoop strains, covering the full range of partial autofrettage pressure and diameter ratios reported in Fig. 1 of [8], are replicated to within 0.5 percent by the current method.

An apparently anomalous effect was noted which helps to explain equivalent variations in strain in a later section. Consider a typical tube of radius ratio, $b/a=2$. Autofrettage pressures were determined for a given level of overstrain with open-end conditions. These, together with additional values covering closed-end and plane strain conditions, are presented in Fig. 5, wherein pressure is normalized using that for Tresca, plane stress, from Eq. (2).

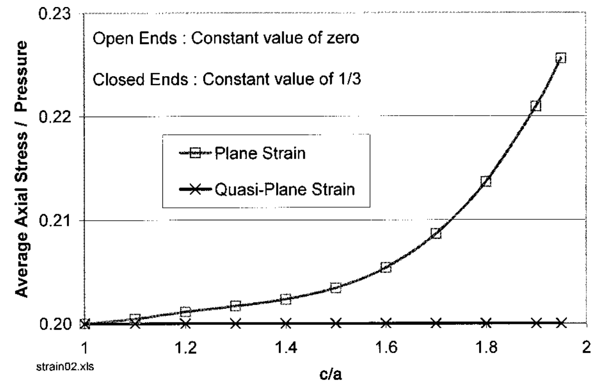

Fig. 6 Average axial stress/autofrettage pressure for plane strain and quasi-plane strain ($b/a=2$)

As expected, the results for plane strain are bounded by the open and closed-end solutions. However, plane strain is not consistently separated from these two bounds, the effect being particularly evident approaching 100 percent overstrain. This is due to subtle differences arising from the fact that, while average axial stress is proportional to autofrettage pressure for open and closed-end solutions, this is not so for plane strain after the onset of yielding. The plane strain solution was compared with an artificial quasi-plane strain (QPS) solution, with constant average axial stress/autofrettage pressure held at the ratio which obtains during the elastic phase. This ensures that prior to the onset of plasticity, plane strain and QPS are identical, but thereafter may differ. Figure 5 shows the pressures for QPS. These results demonstrate a more consistent separation from open and closed-end solutions.

Figure 6 shows the average axial stress for plane strain and for QPS. A maximum difference of 13 percent is evident. Analogous, but not proportional, effects in strain variation are reported in upcoming sections.

Residual Stress Profiles After Pressure Removal

The pressure ratios presented in the previous section provide the pressure necessary to achieve a given percentage overstrain. When the bore pressure defined in Fig. 3 and Eq. (11) is removed residual stresses are ''locked in'' to the tube. It is during this unloading phase that the Bauschinger effect may manifest itself.

Figure 7 relates to the case $b/a=2$ without Bauschinger effect. It shows the percentage error in bore hoop stress and in percent-

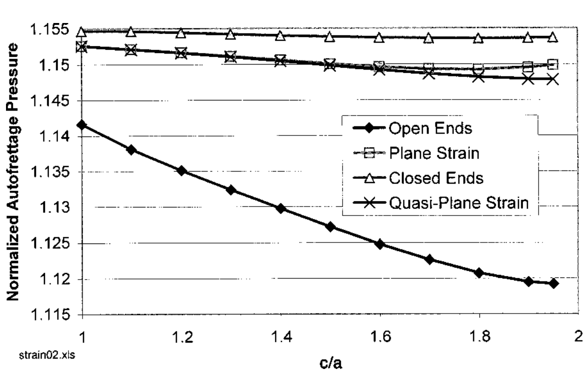

Fig. 5 Pressures at autofrettage peak for plane strain, open-end, and closed-end conditions, $b/a=2$. Results normalized using Eq. (1).

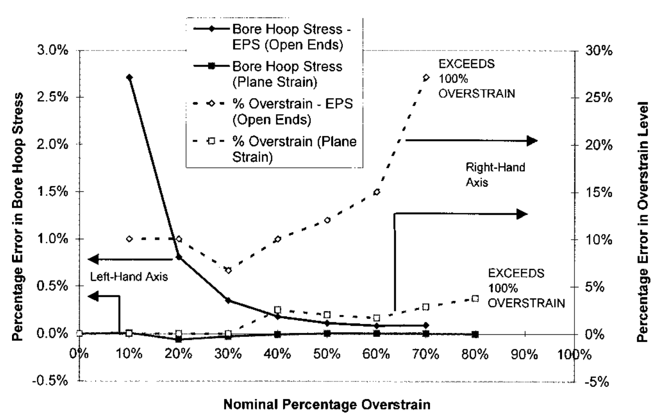

Fig. 7 Percentage error in bore hoop stress and in percentage overstrain resulting from use of Hill's approximation [10]

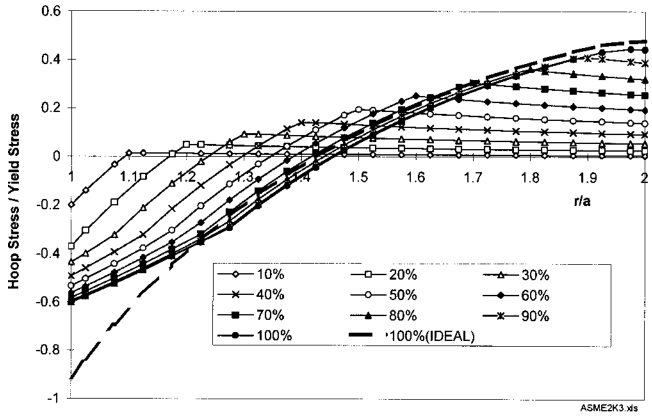

Fig. 8 Hoop residual stress profile for $b/a=2$ with various percentage overstrains; von Mises and engineering plane strain (EPS) conditions assumed

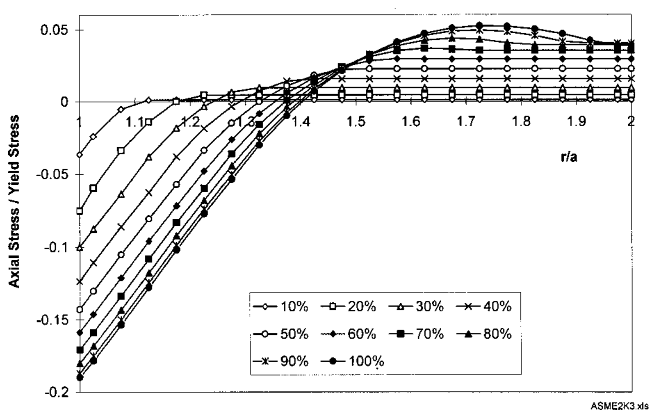

Fig. 9 Axial residual stress profile for $b/a=2$ with various percentage overstrains; von Mises and engineering plane strain (EPS) conditions assumed

age overstrain for both true plane strain and EPS based upon Hill's model [10]. In the case of plane strain Hill's model provides bore hoop stress within 0.1 percent and underestimates overstrain by between 2.5 and 4.0 percent. Equivalent discrepancies in the EPS case are less than 2.7 percent for hoop stress, but with large underestimates in percentage overstrain at higher nominal overstrains.

Figure 8 relates to the case $b/a=2$ including Bauschinger effect. It shows typical residual hoop stress profiles $\sigma_\theta]^{\text{VMEPS}}$ for the full range of possible overstrain. The profile relating to 100 percent overstrain without Bauschinger effect is shown as a heavy broken line; the remainder of the results include Bauschinger effect. Qualitatively, these results are very similar to those for Tresca, plane stress [4] summarized earlier and the observations listed as bullet points in the introduction are unchanged. However, there is some increase in magnitude of residual hoop stress between Tresca, plane stress and von Mises, EPS. Examples of percentage increase in compressive bore hoop stress are 10.3 percent (20 percent overstrain), 11.4 percent (40 percent overstrain), 10.7 percent (60 percent overstrain), 9.4 percent (80 percent overstrain), 8.5 percent (100 percent overstrain).

The associated values of axial stress are presented in Fig. 9. The approximate rule-of-thumb *bore hoop stress×Poisson's ratio =bore axial stress* is observed. Because there is an extremely large number of b/a and overstrain combinations under investigation, results presented hereafter focus upon bore hoop stress values.

Residual Bore Hoop Stresses

It has been noted [13] that percentage plastic strain during initial autofrettage pressurization is of crucial importance. Because this is a strong function of c/a and relatively insensitive to b/a, it is frequently more physically significant to plot hoop stresses as a function of c/a rather than percentage overstrain.

Figure 10 shows a composite plot of bore hoop stress versus c/a. One set is predicted from an ideal, von Mises, EPS, elastic-perfectly plastic analysis without Bauschinger effect (annotated

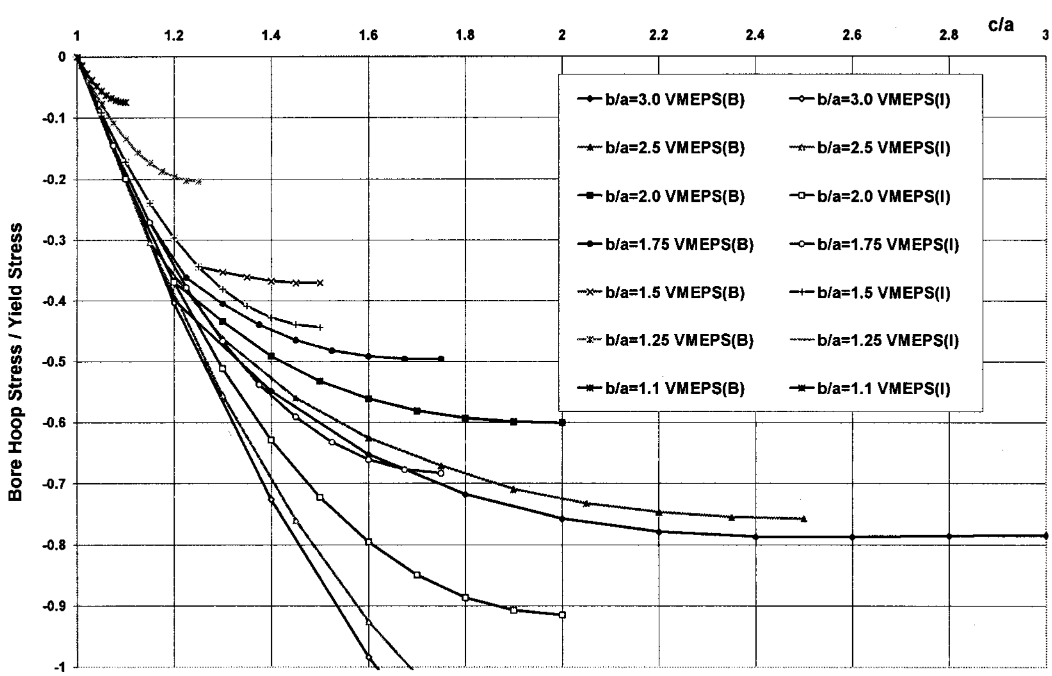

Fig. 10 Bore hoop stress values as a function of c/a for a range of autofrettaged tube geometries. (I) indicates ideal solution, (B) indicates results incorporating Bauschinger effect.

''I'') and the other set from a similar analysis which includes Bauschinger effect (annotated ''B''). In all cases bore hoop stress values are normalized with yield stress.

One design approximation to the Bauschinger effect is that compressive hoop stress at the bore is capped at 70 percent of yield when the ideal value exceeds this level. Figure 10 indicates that this assumption may be significantly nonconservative. For example, an overstrain of 27 percent for $b/a=2.5$ would be capped at 70 percent of yield, whereas its value is only 53 percent of yield. Such an overestimate could produce orders of magnitude shift in fatigue lifetime calculations from pre-existing defects in cyclically pressurized cylinders. However, the use of an approximation based upon 70 percent of the ideal value does give a useful design approximation (within 2 percent and conservative) for $c/a>1.4$.

Figure 10 also indicates a consistent ''cut-off'' at $c/a=1.2$, below which the results follow the ideal curve without Bauschinger effect and above which they exhibit an increasing loss of compressive yield strength arising from the Bauschinger effect. The cut-off is clear for all results with $b/a\geqslant 1.5$. While the effect was more subtle, it is also exhibited in the numerical results for $b/a=1.25$. The Bauschinger effect is absent for $b/a\leqslant 1.2$.

Possible Design Procedure

The data in Fig. 10 may be presented in a useful format which leads to a possible design procedure. Figure 11 shows the same data normalized with $\sigma_\theta]_{\text{bore}}^{T\sigma}$, Eq. (7). Two features emerge:

(a) There is an upper bound (shown as a heavy line) which defines residual stress for those cases in which Bauschinger effect is absent. All ideal curves shown in Fig. 10 fall on a single curve. Deviation from the curve is less than 1 percent over the full range of overstrain and b/a ratios considered.

(b) When Bauschinger effect is present, the residual stress variation is a near-linear function of b/a with generally constant slope for all overstrain levels.

Figure 11 could form the basis of a single, accurate design curve whereby autofrettage pressure for required overstrain is obtained using Eq. (11) and residual stress is obtained via Fig. 11. The procedure involves entering with b/a, moving vertically to appropriate percentage overstrain or bounding curve, whichever is encountered first, and reading off bore hoop stress.

The upper bound of Fig. 11 may be approximated as follows (maximum error 0.5 percent):

$$\sigma_\theta]_{\text{bore}}^{\text{VMEPS}}/\sigma_\theta]_{\text{bore}}^{\text{T}_\sigma}=0.0791(b/a)^3-0.6502(b/a)^2+1.8141(b/a)-0.5484 \tag{15}$$

Because reversed yielding will occur even in the absence of Bauschinger effect when $c/a>2.22$, Eq. (12) is limited to $c/a\leqslant 2.22$. The linear sections which incorporate the Bauschinger effect are approximated by

$$\sigma_\theta]_{\text{bore}}^{\text{VMEPS}}/\sigma_\theta]_{\text{bore}}^{\text{T}_\sigma}=R-0.7086\cdot(1.0296m^3-2.7994m^2+2.6631m-0.89) \tag{16}$$

where

$$R=1.0388-0.1651(b/a) \tag{17}$$

and

$$m=(c-a)/(b-a) \tag{18}$$

This fit is shown for comparison as straight, dotted lines in Fig. 11. Overall the fit is conservative with maximum errors of 5 percent. In the ranges of most practical application, $1.75\leqslant b/a\leqslant 3.0$, $30\ \text{percent}\leqslant(c/a)/(b-a)\leqslant 80\ \text{percent}$, maximum error, again conservative, is generally less than 2 percent.

The overall design procedure (i.e., pressure calculation via Eq. (11) and stress calculation via Eq. (15) or (16)) was compared with the original data presented in Fig. 10. Maximum difference is generally 1.5 percent; this is considered adequate for a simple design procedure.

The upper bound, defined by Eq. (15) was also examined in more detail in order to assess existing models. Figure 12 shows the bound relating to von Mises, EPS based upon Eq. (15), together with the equivalent, numerically determined, bound for von Mises, plane stress; the latter appears to exhibit a limit of $2/\sqrt{3}$ with increasing b/a.

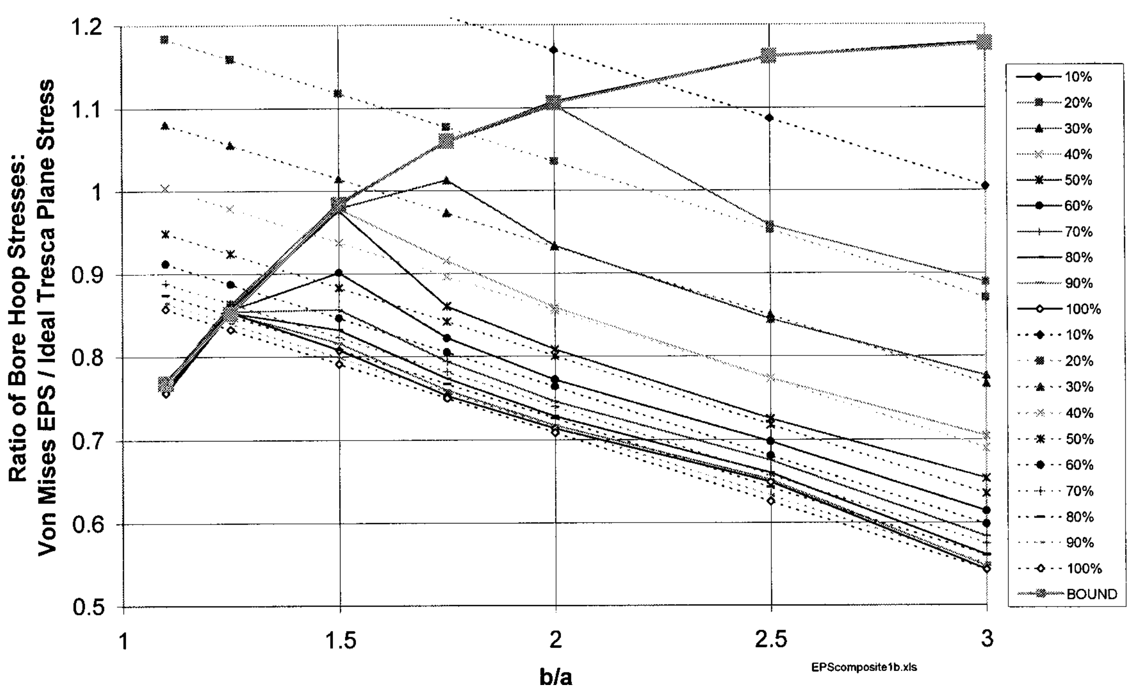

Fig. 11 Ratio of bore hoop stresses, von Mises EPS/ideal Tresca plane stress. Broken lines indicate linear fit to Bauschinger-affected results.

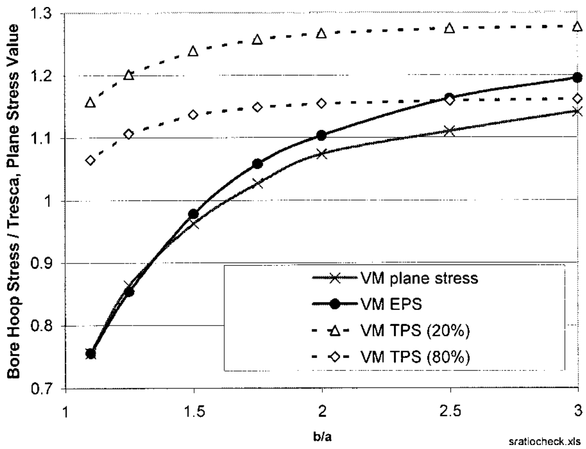

Fig. 12 Bore hoop stresses, von Mises EPS, Tresca EPS, and von Mises TPS, each normalized with Tresca plane stress

In order to further examine Hill's model [10] referred to in the earlier ''Analysis Procedure'' section, the equivalent, numerically determined solutions for the case of von Mises TPS are presented for overstrains of 20 and 80 percent. The maximum difference between these results and the $2/\sqrt{3}$ value proposed by Hill varies between +11 percent (conservative) and −7 percent (nonconservative). It is also apparent, perhaps surprisingly, that von Mises plane stress is a better (and consistently conservative) approximation to von Mises EPS than is von Mises TPS.

ASME Code Comparisons—Pressure

Autofrettage, including Bauschinger effect, is covered by Article KD5 of the ASME Pressure Vessel Code [9] which fully defines the procedure for calculating residual stresses. Points of significance in the Code are:

(a) Autofrettage pressure is defined as $1.15p]^{T\sigma}$ with $p]^{T\sigma}$ defined in Eq. (2).

(b) Residual bore hoop stress in the absence of Bauschinger effect is given by $1.15\sigma_\theta]^{T\sigma}_{\text{bore}}$ with $\sigma_\theta]^{T\sigma}_{\text{bore}}$ defined in Eq. (7).

(c) Section KD-522.2 contains details of correction for Bauschinger effect

(d) The code limits the bore pressure calculation to a maximum of 40 percent overstrain.

Both (a) and (b) are at odds with the conclusions arising from numerical solutions presented herein. However, this does not necessarily invalidate the code since the correction procedure serves to modify residual stress calculations. In order to properly compare the code with the numerical procedure presented herein, it is necessary to follow code procedure precisely.

Figure 13 shows the result of a detailed comparison of code with the von Mises EPS numerical procedure. The results cover the range $1.25 \leqslant b/a \leqslant 3.0$. The case $b/a = 1.1$ is omitted since use of the code autofrettage pressure leads, for all overstrains, to a numerical prediction of greater than 100 percent overstrain. Figure 13 presents percentage differences between bore stress as calculated via the code and that obtained via the von Mises EPS analysis, i.e.,

$$\text{Percent Difference} = \frac{(\text{Code Solution} - \text{Numerical Solution})}{\text{Numerical Solution}} \tag{19}$$

Hence, a negative difference indicates conservatism within the code. These results indicate:

(a) The ASME code appears generally conservative for all levels of overstrain for which it is valid (i.e., up to a maximum of 40 percent).

(b) The code may be nonconservative at very low levels of overstrain (10–20 percent) for diameter ratios >2.0. However, the overestimate is limited to around 5 percent of bore stress.

(c) The code formulation, based upon autofrettage pressure, is not suitable in its present form for use beyond 40 percent overstrain.

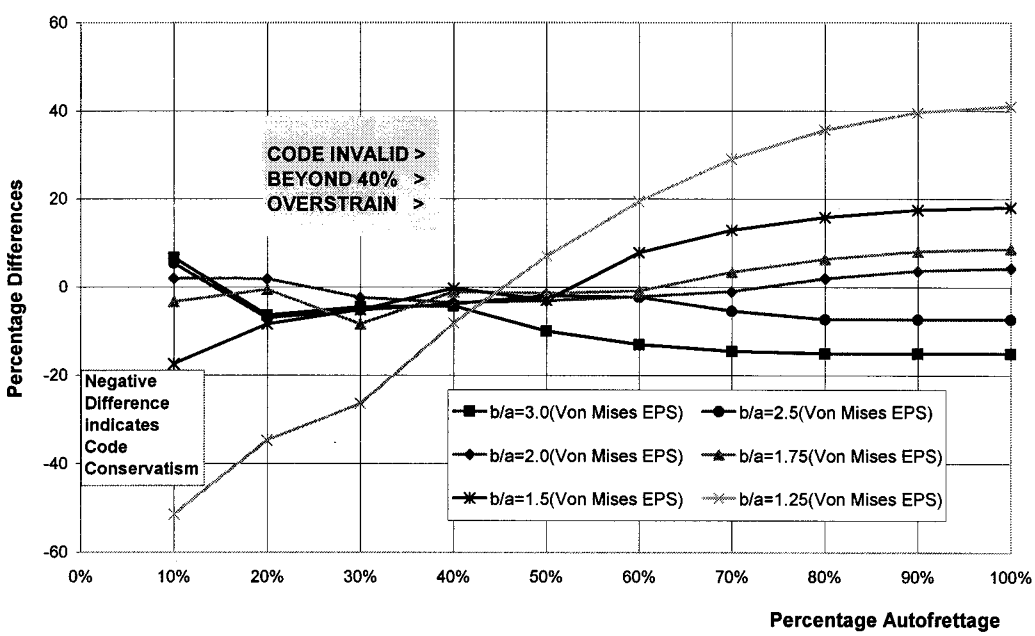

Fig. 13 Percentage difference between ASME Code and von Mises EPS numerical model; negative values indicate code conservatism. Note: code validity limited to 40 percent overstrain.

Strains During Autofrettage Loading

Figure 14 shows normalized bore hoop strain, ε_a, as a function of c/a for each of three end conditions. For numerical reasons errors are likely to be greatest as 100 percent overstrain ($c/a = 2$) is approached; for this reason, a refined node distribution was employed near to the OD.

Results for plane strain are compared with those due to [14], while those for open ends are compared with [15]; there is no discernible difference. No equivalent solution is available for the case of closed ends; however, an alternative comparison is reported in a subsequent section.

Hoop strains in the plastic region of an open-end partially plastic thick cylinder are approximated, with an implied accuracy of 2 percent [7], by

$$\varepsilon_a E/Y = 1.08(1-2\nu)\ln(r/c) + \frac{c^2(1-\nu) - b^2(1-2\nu) + [(c^2b^2)/r^2](2-\nu)}{\sqrt{3b^4+c^4}} \tag{19}$$

Figure 15 shows the result of normalizing the bore hoop strain results in Fig. 14 using Eq. (19) evaluated at $r=a$, this provides an excellent approximation for the open-end case with a maximum discrepancy of 2 percent at 100 percent overstrain. However, Eq. (19) does not appear to be appropriate for the other two cases.

As a further check, Fig. 16 shows a plot of ID strain versus OD strain. There is no discernible difference between the current numerical results and those of Marcal [8], who obtained solutions for open and closed-end conditions. Hence, strain values for each end condition have now been successfully compared with available data from at least one independent source. Figure 16 also shows the anomaly in plane strain predictions at high overstrain analogous to that which was investigated previously; a single QPS value, evaluated at 100 percent overstrain, is shown. Although not reported in detail herein, the effect is less than 0.15 percent prior to 50 percent overstrain, increasing to 1 percent at 100 percent overstrain.

OD hoop strain values are presented in Fig. 17. These are shown in normalized form in Fig. 18. The normalizing strain is the ideal, Tresca, plane stress solution, namely

$$\varepsilon_b = (Y/E)\cdot(c^2/b^2) \tag{20}$$

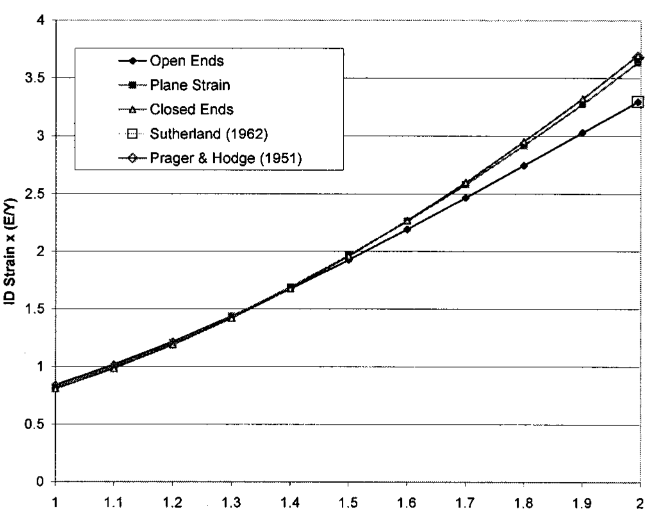

Fig. 14 Bore hoop strain values at autofrettage peak for plane strain, open-end, and closed-end conditions

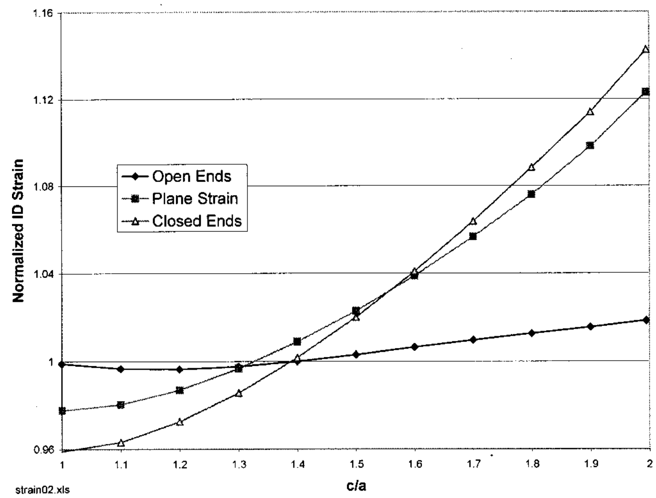

Fig. 15 Bore hoop strain values at autofrettage peak for plane strain, open-end, and closed-end conditions. Results normalized using Eq. (19).

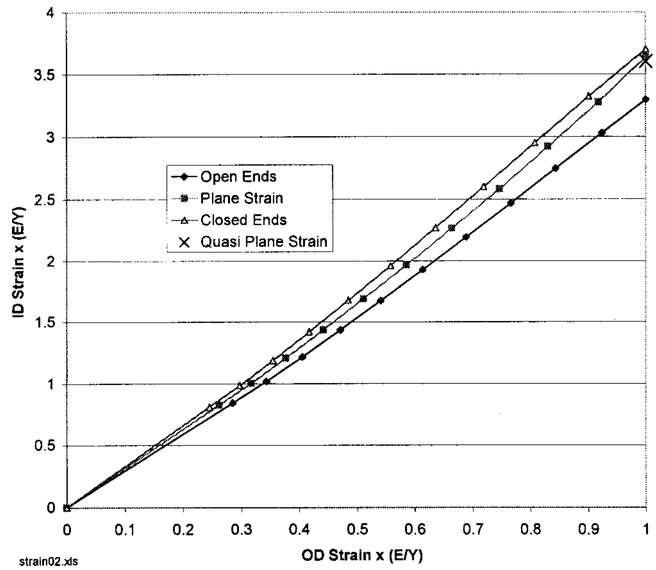

Fig. 16 Bore hoop strain versus OD hoop strain at autofrettage peak for plane strain, open-end, and closed-end conditions. Results for open and closed-end conditions coincide with [8].

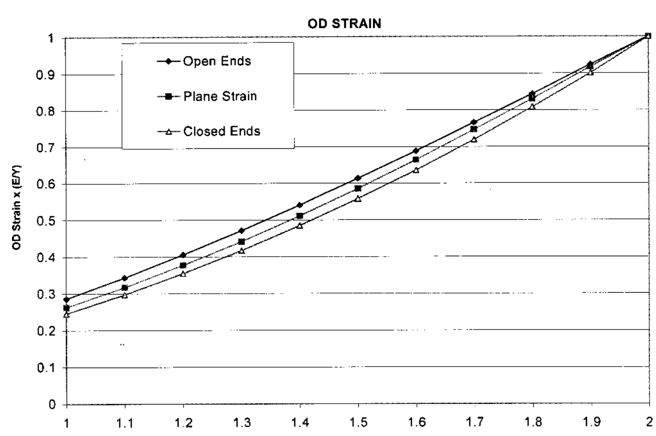

Fig. 17 OD hoop strain values at autofrettage peak for plane strain, open-end, and closed-end conditions

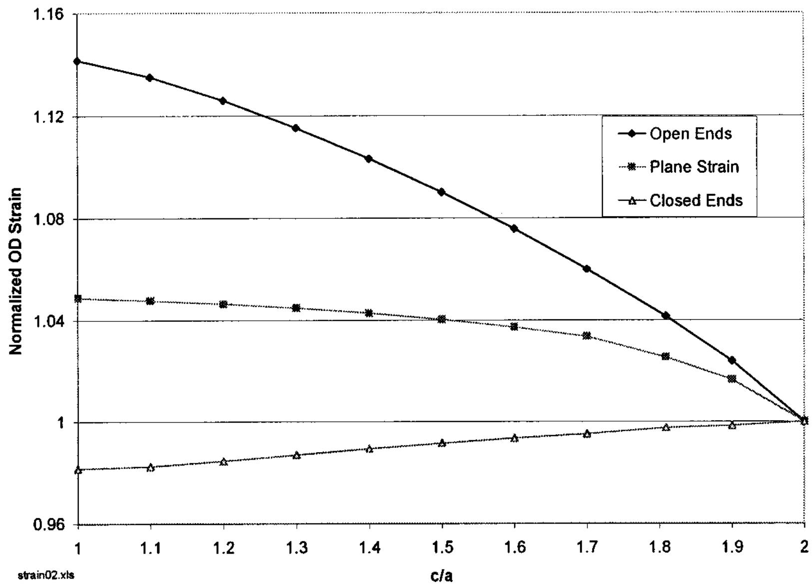

Fig. 18 OD hoop strain values at autofrettage peak for plane strain, open-end, and closed-end conditions. Results normalized using Eq. (20).

Strains During Autofrettage Unloading

The Bauschinger effect serves to reduce the yield strength in compression and produces further yielding during removal of autofrettage pressure. The effect upon residual stress has already been examined in detail. The objective now is to quantify the effect upon residual strain.

ID and OD strains during unloading are shown in Fig. 19 for each of the three end conditions. The results are normalized with those which arise from purely elastic unloading for the appropriate end condition [2], namely

$$\frac{E\varepsilon}{p}=\frac{\alpha+(1+\nu)(b^2/r^2)}{(b^2/a^2-1)} \tag{21}$$

p, the autofrettage peak pressure, is obtained from Fig. 3 and $\alpha=(1-2\nu)$, closed ends, $\alpha=(1-\nu)$, open ends, $\alpha=(1+\nu)(1-2\nu)$, plane strain.

The maximum errors associated with the assumption of elastic unloading are approximately 8 percent for ID strain and 6.3 percent for OD strain.

ASME Code Comparisons—Strains

Autofrettage, including Bauschinger effect, is covered by Article KD5 of the ASME Pressure Vessel Code [9]. The Code offers two separate strain-based methods for assessing percentage overstrain during manufacture and provides a procedure by which the associated residual stresses are computed. Each of these two procedures is now assessed.

OD Hoop Strain at Autofrettage Peak. Figure 20 shows the percentage difference between numerical and code-predicted c/a values for each of the three end conditions. Figure 20 also shows, for the open-end condition, the percentage difference between bore stress as calculated via the code and that obtained via the numerical analysis, i.e.

$$\text{Difference}=\frac{(\text{Code Solution}-\text{Numerical Solution})}{\text{Numerical Solution}} \tag{22}$$

A negative difference indicates conservatism within the code; hence, for all common levels of overstrain (20–75 percent), code

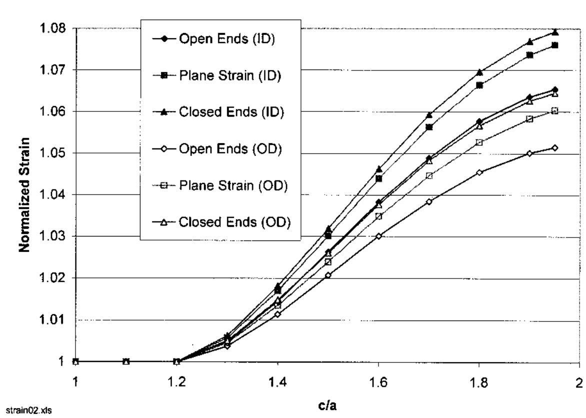

Fig. 19 ID and OD hoop strain values during unloading from autofrettage peak for plane, strain, open-end, and closed-end conditions. Results normalized using Eq. (21).

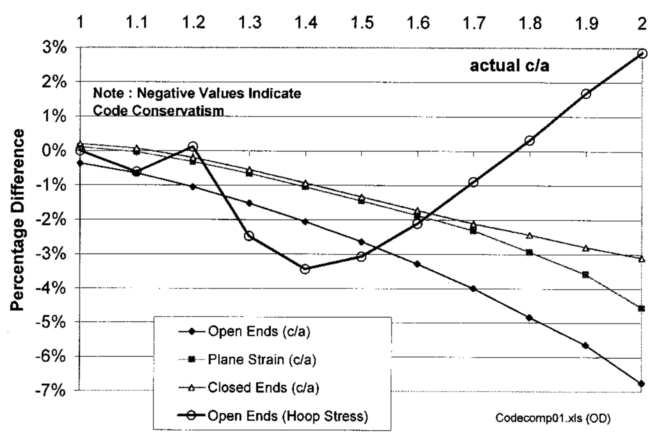

Fig. 20 Percentage difference between code predictions and numerical predictions of c/a and of residual bore hoop stress using OD strain at autofrettage peak

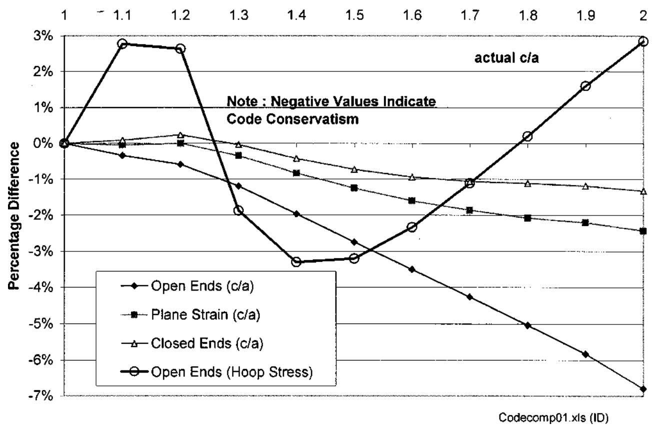

Fig. 21 Percentage difference between code predictions and numerical predictions of *c/a* and of residual bore hoop stress using permanent strain at ID after autofrettage

stress prediction is modestly conservative. Maximum nonconservatism occurs at 100 percent overstrain when the difference reaches 3 percent. There is a straightforward explanation for the apparent discontinuity at 20 percent overstrain; the code incorporates a condition relating to the onset of reversed yielding which produces this effect.

Residual Hoop Strain at Bore after Unloading. In analogous fashion, Fig. 21 shows the percentage difference between numerical and code-predicted c/a values for each of the three end conditions. Figure 21 also shows, for the open-end condition, the percentage difference between bore stress as calculated via the code and that obtained via the numerical analysis. Maximum nonconservatism again occurs at 100 percent overstrain when the difference reaches 3 percent.

Summary and Conclusions

This work extended an existing numerical procedure to calculate a wide range of autofrettage pressures and a limited number of hoop and axial residual stress fields for tubes under open-end (engineering plane strain) conditions using von Mises criterion. A design curve with numerical fit was proposed which allows the open-end pressure results to be replicated to within 0.5 percent.

The practice of using an autofrettage design pressure, for a given overstrain, of 1.15 times the ideal pressure from a Tresca criterion, plane stress analysis is shown to be appropriate for true plane strain, but inappropriate for engineering plane strain (open ends). Residual hoop stresses in the absence of Bauschinger effect are well predicted by the 1.15 factor model for both plane strain and open ends.

A limited number of residual stress profiles were presented for Bauschinger and non-Bauschinger-affected tubes. These confirm earlier observations relating to hoop stress and provide additional profiles for axial residual stress. By focusing upon the value of residual hoop stress at the bore, a design procedure was formulated which provides accurate representation over the practical range of overstrains and of tube diameter ratios. A design curve with numerical fit to an accuracy of 1.5 percent was proposed.

The practice of scaling to 70 percent of the ideal residual hoop stress to represent Bauschinger effect was shown to be a reasonable and conservative assumption at c/a values exceeding 1.4. Conversely, capping at 70 percent of yield strength is inappropriate and nonconservative in many cases.

The numerical procedure was also used to compare residual hoop stress values with the relevant section of the ASME Code. The code is shown generally to be modestly conservative, albeit limited to a maximum of 40 percent overstrain for design based upon a specific pressure.

This work also extended an existing numerical procedure to calculate autofrettage hoop strains at ID and OD for a tube of radius ratio 2 under open-end (engineering plane strain), closed-end, and plane strain conditions using von Mises criterion. These strains were obtained separately during the loading phase and during the unloading phase. The unloading incorporated Bauschinger effect. Strains were compared with available solutions. General agreement was demonstrated, with agreement within 2 percent of an accepted simple formula for strains at the peak of the autofrettage pressure cycle in the case of open ends.

Certain apparently anomalous behavior in the plane strain condition at high levels of overstrain was shown to be associated with variations in average axial stress.

ASME code predictions of percentage overstrain based upon strains at the peak of the autofrettage cycle were generally within 6 percent of numerical predictions. This in turn provided an agreement within approximately 3 percent in residual bore hoop stress calculation. This discrepancy is generally conservative, becoming nonconservative only at overstrain levels exceeding 80 percent.

Strain during removal of autofrettage pressure, in the presence of Bauschinger effect, was also calculated. This showed that the difference in strain during the unloading phase is up to 8 percent (ID) and 6.3 percent (OD) compared with the predictions of elastic unloading. These latter results showed a similar percentage agreement with the ASME Code as in the peak-strain analysis and would permit correction of estimates of percentage overstrain based upon permanent bore enlargement.

It is suggested that adoption of some of the design procedures proposed within this paper would provide ease of use, accuracy, and much extended code validity.

Acknowledgment

The author gratefully acknowledges helpful discussions with Mr. David P. Kendall.

Nomenclature

a, b, c, d, r =	radii defined in Fig. 1
bore =	bore value
EPS =	Engineering plane strain
n =	percentage overstrain
p =	autofrettage pressure
R =	factor defined in Eq. (17)
T =	Tresca criterion
TPS =	true plane strain
$\mathrm{T}\sigma$ =	Tresca criterion, plane stress
VM =	von Mises criterion
$\mathrm{VM}\sigma$ =	von Mises criterion, plane stress
Y =	uniaxial yield stress
α =	factor defined in Eq. (12)
ε =	hoop strain
ν =	Poisson's ratio
σ_θ =	residual hoop stress after autofrettage
$p]_{100\ \mathrm{percent}}^{\mathrm{T}\sigma}$ =	notation example: pressure for 100 percent overstrain with Tresca, plane stress condition

References

[1] Bauschinger, J., 1881, ''Ueber die Veranderung der Elasticitatagrenze und dea Elasticitatamoduls verschiadener Metalle,'' Zivilingenieur, **27**, pp. 289–348.
[2] Chakrabarty, J., 1987, *Theory of Plasticity*, McGraw-Hill, New York, NY.
[3] Jahed, H., and Dubey, R. N., 1997, ''An Axisymmetric Method of Elastic-Plastic Analysis Capable of Predicting Residual Stress Field,'' ASME J. Pressure Vessel Technol., **119**, pp. 264–273.
[4] Parker, A. P., Underwood, J. H., and Kendall, D. P., 1999, ''Bauschinger Effect Design Procedures for Autofrettaged Tubes Including Material Removal and Sachs' Method,'' ASME J. Pressure Vessel Technol., **121**, pp. 430–437.
[5] Milligan, R. V., Koo, W. H., and Davidson, T. E., 1966, ''The Bauschinger Effect in a High Strength Steel,'' ASME J. Basic Eng., **88**, pp. 480–488.
[6] Troiano, E., 1998, private communication.

[7] Davidson, T. E., and Kendall, D. P., 1970, ''Design of High Pressure Containers,'' *Mechanical Behavior of Metals Under Pressure*, Elsevier, H. Pugh, ed., pp. 54–77.
[8] Marcal, P. V., 1965, ''A Note on the Elastic-Plastic Thick Cylinder with Internal Pressure in the Open and Closed-End Condition,'' Int. J. Mech. Sci., **7**, pp. 841–845.
[9] ASME Pressure Vessel and Piping Design Code, 1997, ''Design Using Autofrettage,'' Division 3, Section 8, Article KD-5, pp. 71–73.
[10] Hill, R., 1967, *The Mathematical Theory of Plasticity*, Oxford University Press, Oxford, UK.
[11] Davidson, T. E., Barton, C. S., Reiner, A. N. and Kendall, D. P., 1963, ''Overstrain of High Strength Open-End Cylinders of Intermediate Diameter Ratio,'' *Proc., First International Congress on Experimental Mechanics*, Pergamon Press, Oxford, UK.
[12] Weigle, R. E., 1960, ''Elastic-Plastic Analysis of a Cylindrical Tube,'' Watervliet Arsenal Technical Report WVTRR-6007.
[13] Parker, A. P. and Underwood, J. H., 1998, ''The Bauschinger Effect in Autofrettaged Tubes—A Comparison of Models Including the ASME Code,'' Proc. ASME Pressure Vessels & Piping Conference, San Diego, CA.
[14] Prager, W., and Hodge, P. G., 1951, *Theory of Perfectly Plastic Solids*, J. Wiley & Sons, New York, NY.
[15] Sutherland, C. D., 1962, ''Elastic-Plastic Analysis of a Cylindrical Tube, Part II,'' Watervliet Arsenal Technical Report No. WVT-RR-6205.